

## §19. Studies on Non-constant Potential and Density on Magnetic Surfaces of Helical Nonneutral Plasmas

Himura, H., Yamamoto, Y., Sanpei, A., Masamune, S. (KIT),  
Isobe, M., Okamura, S., Matsuoka, K.

For the first time, we have experimentally verified the variation of space potential  $\phi_s$  and electron density  $n_e$  on magnetic surfaces of helical electron plasmas. The paper explaining the detail of the findings has been published in Phys. Plasmas<sup>1</sup> and other related topics have been reported in Ref. (2).

The data plotted in Fig. 1 (A) are  $\phi_s(z)$  measured with the  $z$ -probe using the high-impedance emissive method. The horizontal axis is  $\Psi^{1/2}$ , where  $\Psi^{1/2} = 0$  and 1 correspond to the  $R_{ax}$  and LCFS, respectively. In experiments presented here,  $R_{ax}$  is fixed at  $r = 101.6$  cm. All data points plotted in Fig. 1 (A) are averaged values for three different series of experiments. At each shot, the value of  $\phi_s$  is determined by time-averaging  $\phi_s(t)$  for 0.2 – 0.5 ms just after the signal curve has risen completely, except at  $\Psi^{1/2} = 0.9$  where data are time-averaged for  $\sim 2$  ms, because taking longer time to rise up. Error bars denote the maximum and minimum values of  $\phi_s(t)$  during the time-average.

Differences between two values of  $\phi_s$  at  $z > 0$  (henceforth  $\phi_{s,u}$ ) and  $\phi_s$  at  $z < 0$  (henceforth  $\phi_{s,d}$ ) on each magnetic surface (at same value of  $\Psi^{1/2}$ ) are observed. This means that  $\phi_s$  is not constant on magnetic surfaces. As is shown from the data, the difference in  $\phi_s$  becomes larger in the outer region of magnetic surfaces. Actually, the difference reaches about 120 V at  $\Psi^{1/2} \sim 0.9$ , while at  $\Psi^{1/2} \sim 0.3$  the difference almost disappears.

Meanwhile, at the 6-U cross-section, the helical magnetic surfaces have been slightly shifted downward with respect to the center of the elliptic chamber wall. The inferred contours of  $\phi_s$  (equi-potential surfaces) from the measured  $\phi_s(z)$  are shifted upward inside  $\Psi^{1/2} \sim 0.8$ , while downward outside  $\Psi^{1/2} \sim 0.8$ , with respect to the contours of constant  $\psi$  (magnetic surfaces).

In this research, the current-voltage ( $I_e$ - $V_p$ ) characteristics are also measured on each magnetic surface with the same emissive probes that are used to measure  $\phi_s$ . From the  $I_e$ - $V_p$  characteristic curve, we have determined the electron temperature  $T_e$ , as will be described. Then, assuming  $I_e \sim en_e v_{th} S$  at  $V_p = \phi_s$ , the electron particle flux  $\Gamma_e$  is obtained as  $\Gamma_e \sim I_e / eS$ , as shown in Fig. 2 (B). Subsequently, the electron density  $n_e$  is calculated. Here,  $v_{th}$  is electron thermal speed and  $S$  is the probe area.

Figure 1 (C) shows  $n_e(z)$  for  $B = 0.9$  kG and  $V_{acc} = -600$  V. Substantial nonuniformity on each magnetic surface is clearly observed. Fitting curves on  $n_e(z)$  are calculated using polynomial

functions and put for reader's convenience. Another significant point is that  $n_e(z)$  has only one crossover point that appears at  $\Psi^{1/2} \sim 0.4$ . Also,  $n_{e,d}$  is always larger than  $n_{e,u}$  outside  $\Psi^{1/2} \sim 0.4$ . This result means that electrons tend to move towards the grounded chamber wall.

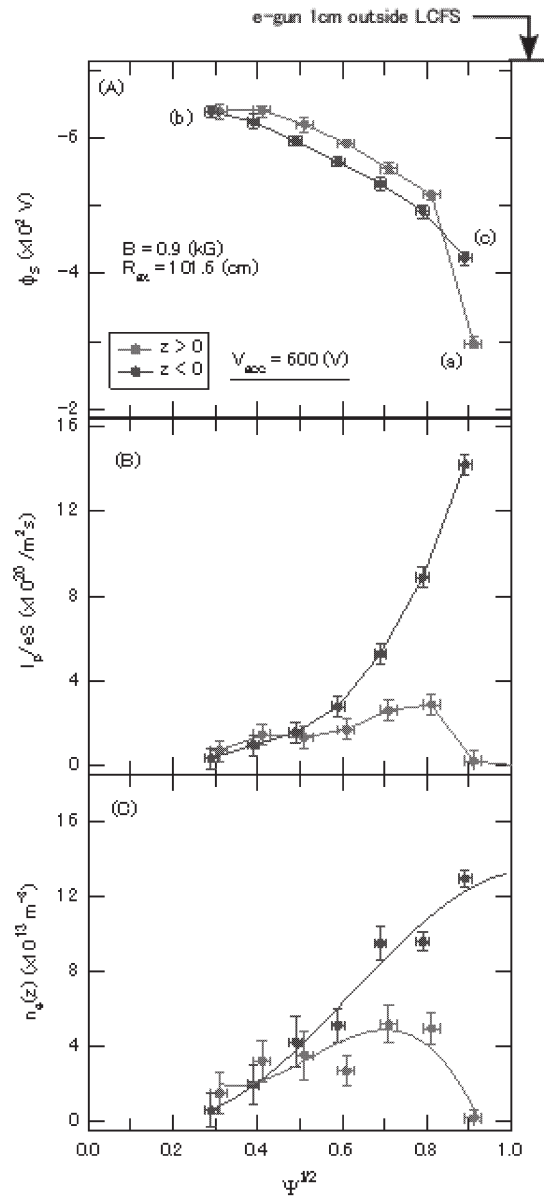


Fig. 1 Profiles of (A) space potential  $\phi_s(z)$ , (B) electron particle flux  $\Gamma_e(z)$ , and (C) electron density  $n_e(z)$  measured at the 6-U cross-section for the case of  $V_{acc} = -600$  V. The horizontal axis is the normalized minor radius. The position of the e-gun is at 1 cm outside the LCFS on a different poloidal cross-section.

- 1) H. Himura *et al.*, Phys. Plasmas **14** (2007) 022507.
- 2) H. Himura *et al.*, Non-Neutral Plasma Physics VI, Vol. **862** (2006) 51.